Performance Analysis of the STAR-RIS-Assisted Downlink NOMA Communication System with MRC

Ugrasen Singh, *Graduate Student Member*, *IEEE*, Hanan Al-Tous, *Senior Member*, *IEEE*, Olav Tirkonnen, *Fellow*, *IEEE*, and Manav R. Bhatnagar, *Senior Member*, *IEEE*

***Abstract*—We discuss a simultaneously transmitting and reflecting-reconfigurable intelligent surface (STAR-RIS)-assisted downlink non-orthogonal multiple access (NOMA) communication system. STAR-RIS employs the energy splitting protocol for transmitting and reflecting the incident signals to users located on different sides of the surface. To study the impact of multiple antennas on the system performance, we perform maximum ratio combining (MRC) at NOMA users and beamforming towards STAR-RIS at the base station (BS). We model the distribution of cascaded Rician fading channels for the proposed system. Closed-form expressions of outage probability, asymptotic outage probability, and system throughput are derived. All theoretically derived results are verified via Monte Carlo simulation.**

***Index Terms*—Maximum ratio combining, non-orthogonal multiple acces, outage probability, beamforming, reconfigurable intelligent surface, system throughput.**

I. Introduction

Reconfigurable intelligent surface (RIS) is introduced to increase the coverage capacity of the wireless networks [1], [2]. However, reflecting-only RIS can provide coverage front side of the surface. To address the limitations of RIS, recently, the concept of simultaneously transmitting and reflecting-RIS (STAR-RIS) has been presented in [3], [4]. The operating principle of STAR-RIS is based on reflection and refraction phenomenon of electromagnetic waves. Elements of STAR-RIS are designed such that incoming radio waves activate time-varying electric and magnetic fields [3]. These time-varying fields can reflect and transmit on either side of the STAR-RIS.

Non-orthogonal multiple access (NOMA) allows multiplexing on the same radio resources by employing superposition coding at the transmitter (Tx) and successive interference cancellation (SIC) at the receiver (Rx). The NOMA users can be ordered in terms of their quality of service (QoS) requirements and STAR-RIS can be employed to realize the corresponding desired order of channel condition [5]. Recently, a research has been triggered towards the design of STAR-RIS assisted NOMA system [6]–[8]. NOMA increases implementation complexity and signaling overhead as compared to orthogonal schemes. However, if NOMA is applied only to clusters of two users, with one user applying SIC, the increase in implementation complexity is kept at a minimum. Further, STAR-RIS-aided single-input single-output (SISO) system for two NOMA users is presented in [6], [7]. Superiority of NOMA over orthogonal multiple access (OMA) schemes is discussed in [8].

In systems where the base station (BS) has multiple antennas, the superiority of NOMA over OMA has been challenged [9]—exploiting the directionality of the channels in beamforming leads to higher gains than combining multiple users to one beam and using NOMA. However, the multiuser-MIMO channel to a set of users served through the same RIS becomes a *keyhole channel* [10], essentially of rank 1, as the BS sees the users through the same keyhole in the form of the RIS. Accordingly, NOMA is a natural multiple access method in a multiuser-MIMO channel with RIS [11]. This is particular so with STAR-RIS, as it is designed to divide radio waves towards two distinct regions, on the two sides of the surface, and thus may serve two users simultaneously. Multiple-input-single-output (MISO) STAR-RIS communication with NOMA has been addressed in [12].

The existing literature on performance analysis for STAR-RIS-assisted downlink NOMA [6]–[8] considers the SISO setup, which is not so much reasonable in the era of massive multiple-input multiple-output (MIMO) communication. To the best of our understanding, theoretical work on statistical distribution modeling of cascaded Rician fading channels for STAR-RIS-assisted MIMO system has not been done so far, which is the main motivation for this work. The main contributions of this work are summarized as follows: 1) We compute the statistical distribution of the cascaded Rician fading channels for STAR-RIS-assisted MIMO system. 2) We present the energy splitting enabled STAR-RIS-assisted wireless network for two NOMA users. The BS applies beamforming to direct the transmit beam towards the RIS and users employ the maximum ratio combining (MRC) to optimally combine the received signals. 3) The outage probability and system throughput are derived theoretically. 4) Asymptotic analysis is also performed to get further insights into the user outage probability in the high signal-to-noise ratio (SNR).

II. System Model

We consider the STAR-RIS-assisted downlink NOMA communication system, where the BS is equipped with N_t transmit antennas and each user has N_r receive antennas. We employ NOMA protocol at the BS to multiplex two users in the same radio resources with different power levels. STAR-RIS is deployed in propagation environment, where a strong line-of-sight (LoS) path exists from the BS. The STAR-RIS splits

This work has been conducted as part of the FICORE (Finnish Indian Consortia for Research and Education) network, supported by the Finnish Ministry of Education and Culture. The work has been supported in part by the Brigadier Bhopinder Singh Chair, Indian Institute of Technology-Delhi, New Delhi, India.

U. Singh, H. A.-Tous, and O. Tirkonnen are with the Department of Information and Communications Engineering, Aalto University, 00076 Espoo, Finland (e-mails: {ugrasen.singh, hanan.al-tous, olav.tirkkonen}@aalto.fi).

M. R. Bhatnagar is with the Department of Electrical Engineering, Indian Institute of Technology Delhi, Hauz Khas, New Delhi 110016, India (e-mail: manav@ee.iitd.ac.in).

incoming signal energy into two parts and then sent with some random phase shifts in the transmission and reflection regions. We assume that the STAR-RIS lies in x-y plane and consists of $N = N_x \times N_y$ reflecting elements with N_x and N_y in the x and y directions, respectively. Since the received signal power is proportional to N^2, the contribution of a direct link between the BS and users on the received signal power can be considered negligible for a large value of N [1, Eq. (7)]. Following the literature [1], [6]–[8], we can neglect the direct link between the BS and the users. Further, the STAR-RIS can be characterized by its diagonal phase shift matrix $\mathbf{\Phi}^{(i)} = \text{diag}\left(\sqrt{\eta_1^{(i)}}e^{-j\phi_1^{(i)}}, \sqrt{\eta_2^{(i)}}e^{-j\phi_2^{(i)}}, \ldots, \sqrt{\eta_N^{(i)}}e^{-j\phi_N^{(i)}}\right)$, where $\eta_n^{(i)} \in (0, 1]$ and $\phi_n^{(i)} \in (0, 2\pi]$ denote the energy splitting coefficient and reflection phase shift of n^{th} reflecting element, respectively, $i \in \{1, 2\}$, and $n \in \{1, 2, \ldots, N\}$. To satisfy the law of energy conservation, energy splitting coefficients must obey the constraint $\eta_n^{(1)} + \eta_n^{(2)} = 1$ [4]. The MIMO channel gain matrix of BS to STAR-RIS link is $\mathbf{H} \in \mathcal{C}^{N \times N_t}$ and STAR-RIS to the users is $\mathbf{G}^{(i)} \in \mathcal{C}^{N \times N_r}$.

A. Channel Model

We assume a strong LoS path between the BS and the STAR-RIS. Generally LoS component is deterministic carries maximum channel power, while the non-line-of-sight (NLoS) components is the random process that cannot be known prior to channel estimation. Therefore, we neglect the NLoS component from the BS to STAR-RIS channel [13]. Then, the channel coefficient of the BS to STAR-RIS channel can be expressed as $\bar{\mathbf{H}} = \sqrt{\rho}\,\mathbf{a}_{\text{RIS}}(\theta_{\text{a}}, \theta_{\text{e}})\mathbf{a}_{\text{BS}}(\theta_{\text{d}})$, where $\rho = \rho_0 d^{-\alpha}$ denotes the path-loss of BS to STAR-RIS channel in which d stands for the distance between BS and STAR-RIS. The path loss at the reference distance d_0 (in kilometer (km)) is denoted by ρ_0 and α is the path loss exponent. An array response vector $\mathbf{a}_{\text{RIS}}(\theta_{\text{a}}, \theta_{\text{e}})$ of an $N_x \times N_y$ uniform rectangular planar array (URPA) at the STAR-RIS can be modeled as [14]

$$\mathbf{a}_{\text{RIS}}(\theta_{\text{a}}, \theta_{\text{e}}) = \Big[1, \ldots, e^{-j2\pi\frac{\delta}{\lambda}(n_x \sin\theta_{\text{e}}\cos\theta_{\text{a}} + n_y\cos\theta_{\text{e}})}, \ldots, e^{-j2\pi\frac{\delta}{\lambda}((N_x-1)\sin\theta_{\text{e}}\cos\theta_{\text{a}} + (N_y-1)\cos\theta_{\text{e}})}\Big]^{\text{T}}, \quad (1)$$

where $0 \le n_x \le N_x - 1, 0 \le n_y \le N_y - 1$, δ is the uniform spacing between STAR-RIS elements and λ is the wavelength, while $\theta_{\text{a}} \in (0,\, 2\pi)$ and $\theta_{\text{e}} \in (0,\, 2\pi)$ indicate the azimuth and elevation angel of arrival (AoA) of signals to the STAR-RIS, respectively. The array steering vector of the N_t uniform linear array (ULA) transmit antennas is

$$\mathbf{a}_{\text{BS}}(\theta_{\text{d}}) = \Big[1, e^{-j2\pi\frac{\tilde{\delta}}{\lambda}\sin\theta_{\text{d}}}, \ldots, e^{-j2\pi\frac{\tilde{\delta}}{\lambda}(N_t-1)\sin\theta_{\text{d}}}\Big], \quad (2)$$

where $\tilde{\delta}$ denotes the antenna spacing and $\theta_{\text{d}} \in (0,\, 2\pi)$ is the angle of departure (AoD) from BS. In addition, we assume that the channel between the RIS and the users is Rician distributed

$$\mathbf{G}^{(i)} = \sqrt{\frac{K_i\,\rho_i}{1+K_i}}\,\bar{\mathbf{G}}^{(i)} + \sqrt{\frac{\rho_i}{1+K_i}}\,\widetilde{\mathbf{G}}^{(i)}, \quad (3)$$

where $\bar{\mathbf{G}}^{(i)}$ and $\widetilde{\mathbf{G}}^{(i)}$ are the LoS and NLoS components, and K_i denotes the Rician K-factor. The path loss is $\rho_i = \rho_0\, d_i^{-\alpha}$, where d_i is the distance between the RIS and user i. The elements of matrix $\widetilde{\mathbf{G}}^{(i)}$ are independent identically distributed (i.i.d.) complex Gaussian random variables with zero mean and unity variance. The LoS component of the STAR-RIS to BS channel can be modeled as $\bar{\mathbf{G}}^{(i)} = \mathbf{a}_{\text{RIS}}(\varphi_{\text{a}}, \varphi_{\text{e}})\mathbf{a}_i(\varphi_{\text{a}}^{(i)})$, where $\varphi_{\text{a}} \in (0,\, 2\pi)$ and $\varphi_{\text{e}} \in (0,\, 2\pi)$ are the azimuth and elevation AoD of signal from the RIS, and $\varphi_{\text{a}}^{(i)}$ is the AoA of signals at user i. The array steering vectors $\mathbf{a}_{\text{RIS}}(\varphi_{\text{a}}, \varphi_{\text{e}})$ and $\mathbf{a}_i(\varphi_{\text{a}}^{(i)})$ can be modeled with (1) and (2).

B. Transmission

We exploit the power-domain NOMA transmission protocol to transmit the superimposed signals of users sharing the same time-slot and frequency band. We assume that the signal at user 1 is stronger than the signal at user 2. The BS superimposes the normalized symbols x_1 and x_2 intended for users 1 and 2, as $x = \sqrt{\beta}\,x_1 + \sqrt{(1-\beta)}\,x_2$, where β is a power allocation coefficient. For the weaker user to be able to decode the signal, more power is allocated to user 2, with $\beta \in (0, 0.5)$. Then the BS transmits the symbol x with total power P_t, measured in units of the noise power spectral density. The received symbol at user i is given by

$$\mathbf{y}^{(i)} = \sqrt{P_t}\,\mathbf{G}^{(i)\text{T}}\mathbf{\Phi}^{(i)}\bar{\mathbf{H}}\mathbf{w}x + \mathbf{n}^{(i)}, \quad (4)$$

where $\mathbf{n}^{(i)} \in \mathcal{CN}(0, \mathbf{I}_{N_r})$ is an additive white Gaussian noise vector at user u_i and $\mathbf{w} \in \mathcal{C}^{N_t \times 1}$ is a beamforming vector. Let us assume that the BS and RIS are fixed, thus the BS-RIS link can be considered a quasi-static fading channel. Therefore, the BS-RIS LoS link can be well-aligned at the BS with $\mathbf{w} = \frac{1}{\sqrt{N_t}}\mathbf{a}_{\text{BS}}^{\text{H}}(\theta_{\text{d}})$. Thus, an equivalent BS-RIS link LoS channel can be expressed as $\mathbf{h} = \bar{\mathbf{H}}\mathbf{w} = \sqrt{\rho\,N_t}\,\mathbf{a}_{\text{RIS}}(\theta_{\text{a}}, \theta_{\text{e}})$. Further, an equivalent cascaded channels gain from BS to user i can be expressed as $\mathbf{f_i} = \mathbf{G}^{(i)\text{T}}\mathbf{\Phi}^{(i)}\mathbf{h}$.

C. Reception

We perform MRC at users to combine the optimally weighted, phase-aligned, and time-synchronized received signal at the receiving antennas. To implement the MRC at user i, an optimal combining vector can be expressed as [15] $\mathbf{v} = \frac{\mathbf{f}_i}{\|\mathbf{f}_i\|^2}$, where $\mathbf{f}_i$ is a column vector of length N_r that contains cascaded BS-STAR-RIS-user channel gains. After employing MRC at user i, the received symbol after MRC is

$$\tilde{y}^{(i)} = \mathbf{v}^{\text{H}}\mathbf{y}^{(i)} = \sqrt{P_t}\,x + \frac{\mathbf{f}_i^{\text{H}}\mathbf{n}^{(i)}}{\|\mathbf{f}_i\|^2}. \quad (5)$$

Further, the strong user 1 performs SIC, and the weak user 2 decodes the signal under interference from the transmission to the other user. When user 1 is attempting to cancel the interference from the transmission to user 2, the pertinent signal-to-interference-plus-noise ratio (SINR) for decoding x_2 at user 1 is

$$\Gamma_{1,2} = \frac{(1-\beta)P_t\,\|\mathbf{f}_i\|^2}{\beta P_t\,\|\mathbf{f}_i\|\,2 + 1}. \quad (6)$$

After SIC at user 1, the received SNR for user 1 signal x_1 can be written as

$$\Gamma_{1,1} = \beta P_t\,\|\mathbf{f}_i\|^2. \quad (7)$$

On the other hand, user 2 decodes its signal x_2 under the interference x_1, the corresponding SINR

$$\Gamma_{2,2} = \frac{(1-\beta)P_t \left\|\mathbf{f}_i\right\|^2}{\beta P_t \left\|\mathbf{f}_i\right\|^2 + 1}. \tag{8}$$

Note that to ensure SIC at user 1, we have to require $\Gamma_{1,2} \geq \Gamma_{2,2}$. This holds always if user 1 has better SNR than user 2.

III. Performance Analysis

A. Distribution of the Cascaded Channel

We present the statistical distribution of the cascade BS-STAR-RIS-user fading channels that are used for outage probability analysis. The norm of the cascaded BS-STAR-RIS-user channel gain can be expressed as $c_i = \left\|\mathbf{f}_i\right\|^2$.

Proposition 1. *The cumulative distributive function (CDF) of c_i can be modeled as*

$$F(c) = 1 - Q_{N_r}\left(\frac{s_i}{\sigma_i}, \frac{\sqrt{c}}{\sigma_i}\right), \tag{9}$$

where $Q_{N_r}(\cdot,\cdot)$ is the generalized Marcum Q-function.

Proof. See Appendix A. ∎

B. Outage Probability

1) Outage Probability of User 1: Based on the NOMA principle, user 1 is not in outage, whenever it can decode both x_2 and x_1. The outage probability of user 1 thus is

$$P_1^{\text{out}} = 1 - \Pr\left(\Gamma_{1,2} > \Lambda_2, \Gamma_{1,1} > \Lambda_1\right), \tag{10}$$

where $\Lambda_2 = 2^{R_2} - 1$ and $\Lambda_1 = 2^{R_1} - 1$ denote the threshold SNRs of the user 2 and user 1, respectively, given the corresponding target rates R_2 and R_1 in bits per second per hertz (bps/Hz). By substituting (6) and (7) into (10), P_1^{out} can be given as

$$P_1^{\text{out}} = \begin{cases} 1 - \Pr(c_1 > \Delta_1), & \text{if} \quad \beta < \frac{1}{\Lambda_2+1} \\ 1, & \text{if} \quad \beta \geq \frac{1}{\Lambda_2+1}, \end{cases} \tag{11}$$

where $\Delta_1 = \max\left(\frac{\Lambda_2}{(1-\beta)P_t - \beta P_t \Lambda_2}, \frac{\Lambda_2}{\beta P_t}\right)$. Using (9), the probability of $c_1 > \Delta_1$ can be obtained as

$$\Pr(c_1 > \Delta_1) = 1 - F(\Delta_1) = Q_{N_r}\left(\frac{s_1}{\sigma_1}, \frac{\sqrt{\Delta_1}}{\sigma_1}\right). \tag{12}$$

2) Outage Probability of User 2: The outage event occurs at user 2 when it cannot decode its own signal x_2 by considering x_1 as an interference signal:

$$P_2^{\text{out}} = \Pr\left(\Gamma_{2,2} \leq \Lambda_2\right). \tag{13}$$

By substituting (8) into (13) this becomes

$$P_2^{\text{out}} = \begin{cases} \Pr\left(c_2 \leq \Delta_2\right), & \text{if} \quad \beta < \frac{1}{\Lambda_2+1} \\ 1, & \text{if} \quad \beta \geq \frac{1}{\Lambda_2+1}. \end{cases} \tag{14}$$

where $\Delta_2 = \frac{\Lambda_2}{P_t(1-\beta(1+\Lambda_2))}$. The probability of $c_2 \leq \Delta_2$ can be obtained as

$$\Pr\left(c_2 \leq \Delta_2\right) = F(\Delta_2) = 1 - Q_{N_r}\left(\frac{s_2}{\sigma_2}, \frac{\sqrt{\Delta_2}}{\sigma_2}\right). \tag{15}$$

C. Asymptotic Outage Probability

To obtain the key insights of the proposed system model, we derive the asymptotic outage probability of user i at high value of SNR, i.e., when $P_t \to \infty$. First we apply the orthogonal polynomial expansion of $F(c)$ [17, Eq. (14)]:

$$F(c) = \sum_{m=0}^{\infty} e^{-\frac{s_i^2}{2\sigma_i^2}} \left(\frac{s_i^2}{2\sigma_i^2}\right)^m \frac{\gamma\left(N_r + m, \frac{c}{2\sigma_i^2}\right)}{m!\ (N_r + m - 1)!}, \tag{16}$$

where $\gamma(\cdot,\cdot)$ is a lower incomplete gamma function. It is noticed from (11) and (15) that for $c = \Delta_i$ and $P_t \to \infty$, $\Delta_i \to 0$ and $\gamma\left(N_r + m, \frac{\Delta_i}{2\sigma_i^2}\right) \approx \frac{1}{N_r+m}\left(\frac{\Delta_i}{2\sigma_i^2}\right)^{N_r+m}$. As further simplification, we take the first term of series representation in (16), then $F(\Delta_i)$ can be written as

$$F(\Delta_i) = \frac{1}{N_r!}\, e^{-\frac{s_i^2}{2\sigma_i^2}} \left(\frac{1}{2\sigma_i^2}\right)^{N_r} (\Delta_i)^{N_r}. \tag{17}$$

From (11), (12), and (15), the asymptotic outage probability of user i can be given by

$$\hat{P}_i^{\text{out}} = \begin{cases} \frac{1}{N_r!}\, e^{-\frac{s_i^2}{2\sigma_i^2}} \left(\frac{1}{2\sigma_i^2}\right)^{N_r} (\Delta_i)^{N_r}, \text{if} \quad \beta < \frac{1}{\Lambda_2+1} \\ 1, \qquad\qquad\qquad\qquad\quad \text{if} \quad \beta \geq \frac{1}{\Lambda_2+1}. \end{cases} \tag{18}$$

It is noticed from (11) and (15) that Δ_i is inversely proportional to P_t. At high SNR regime, the outage probability $\hat{P}_i^{\text{out}}$ can be approximated as $(\mathcal{G}_a \times \text{SNR})^{-\mathcal{G}_d}$, where $\text{SNR} = P_t$, $\mathcal{G}_d$ denotes the diversity order, defined as the slope of the asymptotic $\hat{P}_i^{\text{out}}$ curve, whereas $\mathcal{G}_a$ denotes the array gain, defined as the shift of the asymptotic $\hat{P}_i^{\text{out}}$ relative to the reference curve of $P_t^{\mathcal{G}_d}$. Therefore, the diversity order and array gain of the proposed system are $\mathcal{G}_d = N_r$ and $\mathcal{G}_a = 2\sigma_i^2 \left(N_r!\right)^{\frac{1}{N_r}} e^{\frac{s_i^2}{2\sigma_i^2 N_r}}$. Note that N is not affecting the diversity degree – here the RIS is used as a passive element creating a rich scattering environment, we do not assume RIS beamforming based on channel state information. The expected sum throughput of the proposed STAR-RIS-assisted NOMA system, with fixed target rates and corresponding outage probabilities is

$$\tau = (1 - P_2^{\text{out}})R_2 + (1 - P_1^{\text{out}})R_1. \tag{19}$$

IV. Numerical Results and Discussion

This section provides numerical results based on theoretical analysis of outage probability and system throughput for the proposed STAR-RIS-assisted NOMA system. Monte Carlo simulations (shown by markers) validate all theoretically derived results for 10^6 channel realizations. We assume the system parameters as $\delta = \tilde{\delta} = \frac{\lambda}{2}, K_i = 2, \alpha = 2.3, \rho_0 = 1, d_0 = 1\,\text{km}$, and $\eta_n^{(i)} = 0.5$ for all elements.

In Fig. 1, we depict the outage probability of users 1 and 2 versus P_t for $N_r = N_t = 2$ and various values of N, β, and R_i for the proposed scheme. As expected, the outage probability of users improves with increasing N. For $N = 80$ and $R_i = 1$ bps/Hz, the outage probability of user 1 decreases as β increases from 0.2 to 0.3 because the received SNR corresponds to x_1 increases, while the outage probability of user 2 increases because the received SINR corresponds

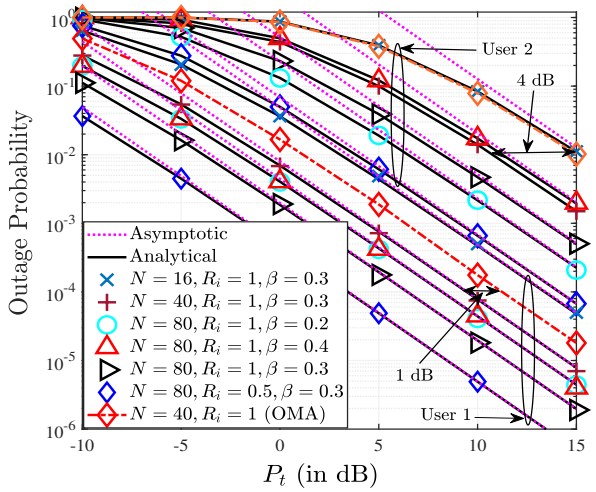

Fig. 1. Outage probability of user 1 and user 2 versus P_t plots for $N_t = N_r = 2, d_1 = d_0$, and $d_2 = 4\,d_0$.

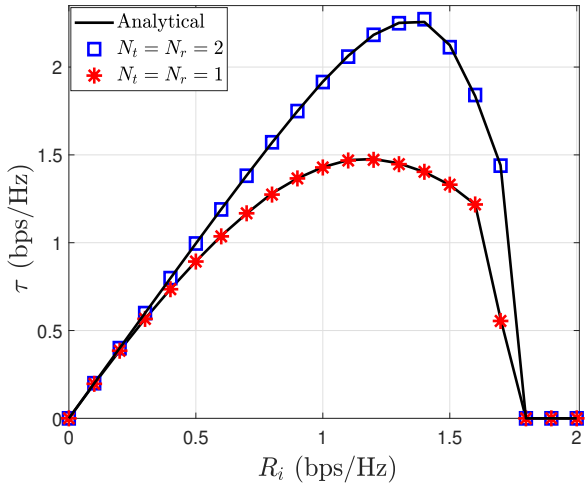

Fig. 3. Expected system throughput versus R_i plots with $d_1 = d_0, d_2 = 4\,d_0, \beta = 0.3, N = 16$ and $P_t = 10$ dB.

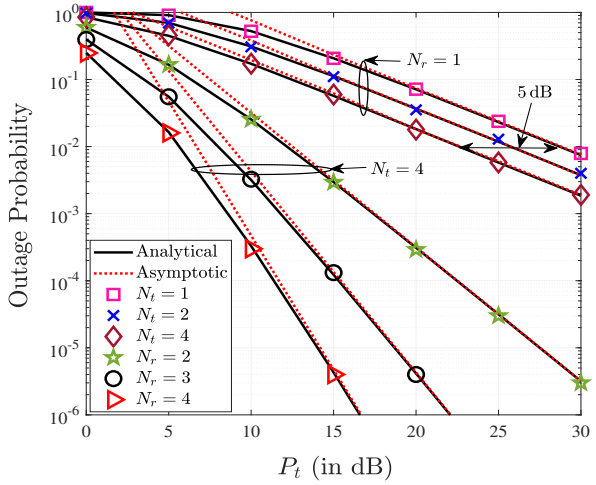

Fig. 2. Outage probability of user u_2 versus P_t plots for different values of N_t and N_r and $d_1 = d_0, d_2 = 4\,d_0, R_i = 1$ bps/Hz, $\beta = 0.3$, and $N = 16$.

to x_2 reduces. As β further increases from 0.3 to 0.4, the outage probability of user 1 and user 2 increase because the probability of SIC and received SINR decrease, respectively. We show a fair comparison between proposed scheme and frequency division based OMA scheme. For $N = 40, R_i = 1$ bps/Hz and $\beta = 0.3$, it can be observed from Fig. 1 that the NOMA outperforms over OMA at the both users.

In Fig. 2, we study the impact of the number Rx and Tx antennas. Without loss of generality, we concentrate on user 2. The outage probability versus P_t plots of user 2 are depicted for $N = 16, \beta = 0.3$, and $R_2 = 1$ bps/Hz. The outage probability improves with increasing N_t. For $N_r = 1$, when N_t increases from 1 to 4, user 2 requires 5 dB less P_t for outage probability of 10^{-2}. This reflects the Tx array gain due to beamforming at BS. When increasing N_r, the slope of outage probability increases linearly, as predicted by (18). This is a result of MRC at the Rx. The simulations perfectly reproduce the analytical outage probability result, verifying that the MIMO STAR-RIS can achieve maximum diversity order N_r due to MRC at the user side.

Fig. 3 illustrates the system throughput versus R_i plots for different values of N_t and N_r. With the increasing values of R_i, the system throughput increases linearly toward the maximum value and then approaches towards to zero. It is seen from the figure that the maximum value of τ improves with increasing N_t and N_r. The expected system throughput versus β plots are demonstrated in Fig. 4 for $N = 16$ and different values of R_i. For $P_t = 10$ dB and $N_t = N_r = 1$, the presented STAR-RIS NOMA system attains maximum throughput 1.6 at $\beta = 0.12$ for $R_1 = R_2 = 1$ bps/Hz, while for $R_1 = R_2 = 2$ bps/Hz it attains maximum throughput 1.8 at $\beta = 0.1$. Noticed from Fig. 4 as the target rates of users increase, desirable value of β shifted towards the origin. Moreover, an optimal value of β can be obtained by maximizing system throughput subject to $\eta_n^{(i)}$ and P_t. As we have seen from the figure that the desirable value of β lies between 0 to 0.5 of the presented system for the given setup. In addition, Fig. 5 depicts the system throughput versus energy splitting coefficient $\eta_n^{(1)} = \eta^{(1)}$ curves for different values of β to examine the effect of the energy splitting coefficient on system performance. For $N_t = N_r = 1, R_i = 1$ bps/Hz, and $\beta = 0.1$, the desirable value of $\eta^{(1)}$ is around 0.5 to attain maximum throughput. Further, when β increases from 0.1 to 0.2, the desirable value of $\eta^{(1)}$ approaches to 0.3. It is seen from the figure that β and $\eta^{(1)}$ are varied inversely proportionally to achieve maximum throughput for the presented system.

V. Conclusions

We have presented the MIMO STAR-RIS-assisted downlink NOMA system to multiplex signals to two users located in the reflection and refraction region of the RIS. We performed MRC at users to achieve receive diversity and designed the beamforming at BS steer the signal towards the STAR-RIS. The probability density function for the cascaded Rician fading channels is modeled theoretically and validated with

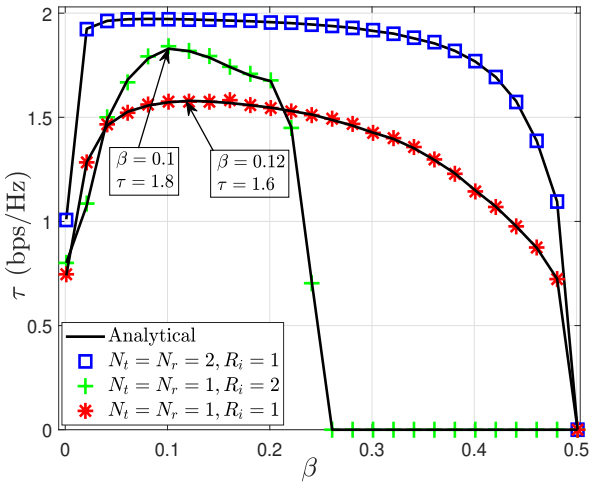

Fig. 4. Expected system throughput versus β plots for $P_t = 10$ dB, $N = 16$, $d_1 = d_0$, and $d_2 = 4\,d_0$.

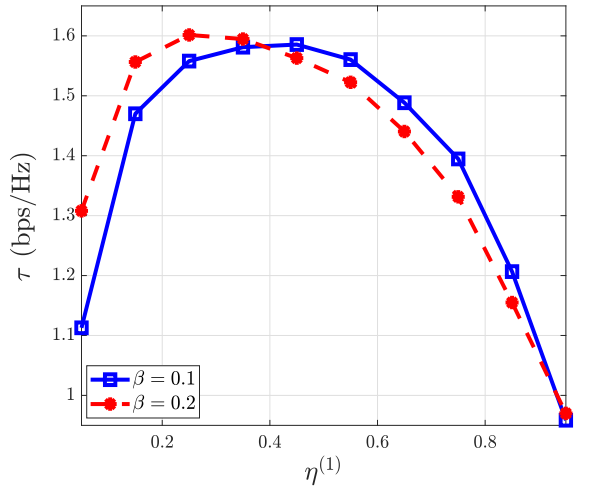

Fig. 5. Expected system throughput versus $\eta^{(1)}$ plots with $d_1 = d_0, d_2 = 4\,d_0$, $N = 16$, $N_t = N_r = 1$, $R_i = 1$ bps/Hz and $P_t = 10$ dB.

Monte Carlo simulation. The outage probability and system throughput are derived on cascaded Rician fading channel. Numerical results reveal how multiple antennas at Tx and Rx can remarkably improve the system throughput. In future work, we will do the performance analysis of the presented system with imperfect CSI at users. The presented work can be extended to a multi-user scenario, where multiplexing and decoding order of user symbols would be in line with conventional NOMA.

Appendix A

From (III-A), c_i can be written as

$$c_i = \left(c_i^{(1)}\right)^2 + \left(c_i^{(2)}\right)^2 + \ldots + \left(c_i^{(r)}\right)^2 + \ldots + \left(c_i^{(N_r)}\right)^2, \quad (20)$$

where $c_i^{(r)} = |\sum_{n=1}^{N} g_{n,r}^{(i)} \sqrt{\eta_n^{(i)}}\, e^{j\phi_n^{(i)}} h_n|, r = 1, \ldots, N_r, g_{n,r}^{(i)}$ is the n^{th} row and r^{th} column element of $\mathbf{G}^{(i)}$, and h_n is the n^{th} element of $\mathbf{h}$. Alternatively, we can write $g_{n,r}^{(i)} = \mathcal{N}(\mu_{n,r}^{(i)}, \Omega_i) + j\mathcal{N}(0, \Omega_i)$, $\mathcal{N}(\cdot)$ stands for normal Gaussian distribution with mean $\mu_{n,r}^{(i)} = \sqrt{\frac{K_i \rho_i}{1+K_i}}\, \bar{g}_{n,r}^{(i)}$, $\bar{g}_{n,r}^{(i)}$ is the n^{th} row and r^{th} column element of $\bar{\mathbf{G}}^{(i)}$ and variance $\Omega_i = \frac{\rho_i}{2(1+K_i)}$. Further, c_i can be expressed as

$$c_i = |\mathcal{N}(\mu_r^{(i)}, \sigma_i^2) + j\mathcal{N}(0, \sigma_i^2)|, \quad (21)$$

where variance $\sigma_i^2 = \Omega_i \sum_{n=1}^{N} |\sqrt{\eta_n^{(i)}}\, e^{j\phi_n^{(i)}} h_n|^2$ and mean $\mu_r^{(i)} = \sum_{n=1}^{N} \mu_{n,r}^{(i)} \sqrt{\eta_n^{(i)}}\, e^{j\phi_n^{(i)}} h_n$. From (20) and (21), it is observed that the c_i has non-central chi-square distribution with $2N_r$ degree of freedom and $s_i^2 = \sum_{r=1}^{N_r} |\mu_r^{(i)}|^2$ non-centrality parameter [16], is as follows:

$$f(c_i) = \frac{1}{2\sigma_i^2} \left(\frac{c_i}{s_i^2}\right)^{\frac{N_r - 1}{2}} \exp\left(-\frac{c_i + s_i^2}{2\sigma_i^2}\right) I_{N_r - 1}\left(\frac{\sqrt{c_i} s_i}{\sigma_i^2}\right), \quad (22)$$

where $c_i > 0$. The CDF of c_i can be written as $F(c) = \Pr(c_i \leq c)$, which is given in $Proposition 1$.

References

[1] E. Basar, M. D. Renzo, J. D. Resny, M. Debbah, M. S. Alouini, and R. Zhang,"Wireless communication through reconfigurable intelligent surfaces," *IEEE Access,* vol. 7, pp. 116753–116773, August. 2019.

[2] E. Arslan et al., "Over-the-air equalization with reconfigurable intelligent surfaces,"*IET Commun.*, vol. 16, no. 13, pp. 1486–1497, May 2022.

[3] X. Mu, Y. Liu, L. Guo, J. Lin, and R. Schober, "Simultaneous transmission and reflection (STAR) RIS aided wireless communication," *IEEE Trans. Wirel. Commun.*, vol. 21, no. 5, pp. 3083–3098, May 2022.

[4] H. Zhang et al., "Intelligent omni-surfaces for full-dimensional wireless communications: Principles, technology, and implementation" *IEEE Commun. Mag.*, vol. 60, no. 2, pp. 39–45, Feb. 2022.

[5] Y. Liu et al., "Evolution of NOMA Toward Next Generation Multiple Access (NGMA) for 6G," *IEEE Journal on Selected Areas in Communications*, vol. 40, no. 4, pp. 1037–1071, April 2022.

[6] C. Zhang, W. Yi, K. Hany, Y. Liu, Z. Dingz, and M. D. Renzo, "Simultaneously transmitting and reflecting RIS aided NOMA with randomly deployed users," in *Proc. IEEE Global Commun. Conf. (GLOBCOM),* Madrid, Spain (Virtual), Dec. 2021, pp. 1–6.

[7] T. Wang, M.-A. Badiu, G. Chen, and J. P. Coon, "Outage probability analysis of STAR-RIS assisted NOMA network with correlated channels," *IEEE Commun. Lett.*, vol. 26, no. 8, pp. 1774–1778, Aug. 2022.

[8] C. Wu, Y. Liu, X. Mu, X. Gu, and O. A. Dobre, "Coverage characterization of STAR-RIS networks: NOMA and OMA," *IEEE Commun. Lett.*, vol. 25, no. 9, pp. 3036–3040, Sep. 2021.

[9] B. Clerckx et al., "Is NOMA efficient in multi-antenna networks? A critical look at next generation multiple access techniques," *IEEE Open Joun. Commun. Society*, vol. 2, pp. 1310–1343, Jun. 2021.

[10] S. Loyka and A. Kouki, "On MIMO channel capacity, correlations, and keyholes: analysis of degenerate channels," *IEEE Trans. Commun.*, vol. 50, pp. 1886–1888, Dec. 2002.

[11] G. Yang, X. Xu, Y. C. Liang and M. D. Renzo, "Reconfigurable intelligent surface-assisted non-orthogonal multiple access," *IEEE Trans. Wirel. Commun.*, vol. 20, no. 5, pp. 3137–3151, May 2021.

[12] J. Zuo, Y. Liu, Z. Ding, L. Song, and H. V. Poor, "Joint design for simultaneously transmitting and reflecting (STAR) RIS assisted NOMA systems," *IEEE Trans. Wirel. Commun.*, Aug 2022.

[13] W. Ma, L. Zhu, and R. Zhang, "Passive beamforming for 3-D coverage in IRS-assisted communications," *IEEE Commun. Lett.*, vol. 11, no. 8, pp. 1763–1767, Aug. 2022.

[14] A. Wang, R. Yin, and C. Zhong, "Channel estimation for uniform rectangular array based massive MIMO systems with low complexity," *IEEE Trans. Veh. Techn.*, vol. 68, no. 3, pp. 2545–2556, 2019.

[15] E. G. Larson and P. Stoica, "Space-time block coding for wireless communications," *Cambridge University Press*, New York, 2008.

[16] M. K. Simon, "Probability distributions involving gaussian random variables: A handbook for engineers and scientists," *Berlin, Germany: Springer*, 2006.

[17] S. Andras, A. Baricz, and Y. Sun, "The generalized Marcum Q-function: an orthogonal polynomial approach," *Acta Univ. Sapientiae, Mathematica*, vol. 3, no. 1, pp. 60–76, 2011.